BioMetals **17:** 145–155, 2004.

Characterization and metal affinity of Tirofiban, a pharmaceutical compound used in acute coronary syndromes

E. Ferrari, L. Menabue & M. Saladini*
*Università degli Studi di Modena e Reggio Emilia, Dipartimento di Chimica, Via Campi, 183 41100 Modena (Italy); *Author for correspondence (E-mail: saladini@unimore.it*

Received 7 May 2003; accepted 11 July 2003. Published online: January 2004

Key words: crystal structure, metal-complexes, Tirofiban

Abstract

The crystal and molecular structure of Tirofiban [N-(n-butanesulfonyl)-O-(4-(4-piperidinyl)-butyl)-(S)-tyrosine] is here reported. In the solid state the carboxylic group is in the anionic form while the piperidine molecule appear in the protonated form. By H NMR spectroscopy and potentiometric study three pK_a are found: $pKa_{COOH} = 3.1(1)$, $pKa_{NHPIP} = 11.6(1)$ and $pKa_{NHSO2} = 13.8(1)$. The complexing ability of Tirofiban towards various metal ions (Cu(II), Ni(II), Co(II), Cd(II), Pb(II), Zn(II) and Ca(II)) is also determined by means of potentiometric studies. The prevailing species are $[M(TirH)_2]^{2+}$ where the ligand coordinates the metal ion through carboxylic group, while the piperidine nitrogen is still protonated. The great stability of these complexes may be due to the presence of hydrogen bond interactions, as well as the formation of stacking interactions involving the phenyl ring of the tyrosine residue.

Introduction

Platelet-fibrogen interaction is a key step in the pathogenesis of coronary artery thrombosis. Fibrogen, by binding to several glycoprotein IIb/IIIa receptors simultaneously causes cross-linking of platelets and promotes platelet accumulation and thus thrombus formation (Van de Werf 1997; Ferguson *et al.* 1998). Variable inibition levels of GPIIb/IIIa function may occur after administration of various GPIIb/IIIa antagonists (Mousa *et al*. 2000). Anti-platelet efficacy of GPIIb/IIIa antagonists is significantly effected by changes of plasma $[Ca^{2+}]$ levels, in particular the presence of an anticoagulant such as citrate, which chelates calcium, enhances the potency of certain GPIIb/IIIa antagonists (Kereiakes *et al.* 2001).

Tirofiban, a nonpeptide tyrosine derivative, is an intravenously administered non peptide GPIIb/IIIa receptor antagonist that specifically inhibits fibrogen-dependent platelet aggregation and prolongs bleeding time in patients with acute coronary syndromes (McClellan *et al*. 1998); it is one of three GP IIb/IIIa antagonists approved by the US Food and Drug Administration for the treatment of patients with acute coronary syndromes (Kazunao *et al.* 2002). Tirofiban [N-(n-butanesulfonyl)-O-(4-(4-piperidinyl)-butyl)-(S)-tyrosine] (Scheme 1) was synthesised by N-sulfonylation of (S)-tyrosine and successive phenolic O-alkylation of the N-protected derivative with a 48% overall yield from tyrosine (Chung *et al.* 1993). The aim of this work is to define the metal legating ability of Tirofiban in order to better understand the role of metal ions in the biological activity of this drug. Our previous study on metal coordination by N-protected amino acids led to the conclusion that the substitution of a $Ar\text{-}SO_2$ group on the amino nitrogen increases the acidic character of sulfonamide nitrogen and the binding mode of such amino acids switches from carboxylate type coordination at low pH to an N,O-chelate coordination (*via* carboxylic oxygen and deprotonated sulfonamidic nitrogen) at higher pH (Saladini *et al*. 2001; Saladini *et al.* 2000). When the protecting group is a carbonyl, such as in N-benzoylglycine, the amino acid undergoes nitrogen deprotonation only in presence of Pb^{2+} ion (Battistuzzi *et al.* 1996). In Tirofiban the tyrosine ni-

trogen atom is protected by a butanesulfonyl group so it seems interesting to verify if this N-protecting group influences the dissociation of the sulfonamidic proton enabiling it to coordinate metal ions. In addition a third potential metal-ligating site is present in Tirofiban, i.e., piperidine nitrogen, which was often found to coordinate metal ions.

The crystal and molecular structure of Tirofiban is here reported together with an H NMR study. The complexing ability of Tirofiban towards various metal ions of biological relevance (Ca(II), Cu(II), Ni(II), Co(II), Zn(II)) and toxic metal ions (Cd(II), Pb(II), Hg(II)) is also determined by means of potentiometric studies. The poor solubility of the metal complexes and the formation of hydroxo-species prevent the study at high pH. The solid complexes are also characterized by means of IR spectroscopy.

Materials and methods

Crystals of Tirofiban useful for x-ray analysis were obtained recrystalizing from water Tirofiban monohydrochloride monohydrate (L-700,462-006x) supplied by Merk & CO. INC Rahway, New Jersey, the measured pH was 4.

Preparation of the solid complexes

$[Hg(Tir)_2] \cdot 2HCl$ (Tir = Tirofiban in the monoanionic form) An aqueous solution of $Hg(NO_3)_2$ (5 ml 0.1 M) was added under continuous stirring to 50 ml of a solution (0.02 M) of Tirofiban at pH 12. A solid microcrystalline compound was rapidly separated at pH 5. Found: C, 45.0; H, 6.6; N, 4.8. Calculated for $C_{44}Cl_2H_{72}HgN_4O_{10}S_2$: C, 45.7; H, 6.3; N, 4.9.

$[Cd(Tir)_2] \cdot 2HCl$ was separated from the solutions implied in the potentiometric titrations in the M/L 1:2 and 1:4 molar ratio at pH 8. Found: C,49.2; H,5.4; N, 6.7 Calculated for $C_{44}CdCl_2H_7N_4O_{10}S_2$: C, 49.5; H, 6.8; N, 5.2.

All attempt to separate the solid complexes with the other metals was unsuccessful owing to the poor solubility of Tirofiban at neutral or acid pH, while at more basic pH the precipitation of the metal hydroxides occurs.

Potentiometry

A Tirofiban-hydrochloride aqueous solution (2×10^{-3} M) was prepared and its concentration was determined potentiometrically. The concentration of *M(II)* nitrate hydrate (C. Erba) was obtained by means of Spectroflame D ICP plasma spectrometer; the sample contained 1% of HNO_3. Potentiometric measurements were performed in aqueous solution at 25±0.1 °C using fully automated ORION 960 Autochemistry System and following the general procedures reported previously (Borsari *et al.* 1999). A constant ionic strength of 0.1 M (solid $NaNO_3$) and nitrogen atmosphere were maintained in all experiments. The stability constants (β_{pqr}), which are defined by eq. 1 and 2 where *M* is the metal, L is the ligand in the completely dissociated form and H is the proton, were refined using the computer program HYPERQUAD (Gans *et al.* 1996)

$$pM + qL + rH \leftrightarrow M_pL_qH_r \quad (1)$$

$$\beta_{pqr} = [M_pL_qH_r]/[M]^p[L]^q[H]^r \quad (2)$$

The protonation constants of Tirofiban were determined by titration of at lest four solutions ($2 \cdot 10^{-3}$ M). The starting solution for each titration of the *M(II)*-containing system was prepared by successive additions of a known volume of $M(NO_3)_2$ and Tirofiban solutions in the metal to ligand molar ratios 1:1, 1:2, 1:4. The metal concentration in the starting solution varied in the range $1 \times 10^{-4} - 1 \times 10^{-5}$. For all the *M(II)*-containing systems, at least 10 measurements were performed, with 40 data points in each titration in the pH range 2.5–10.

X-ray analysis

Intensity data were collected at room temperature (293 K) by using Mo-Kα radiation ($\lambda = 0.71069$) on Enraf-Nonius CAD4 diffractometer using ω-2θ scan technique. Crystal data and details are summarized in Table 1. The data were corrected for Lorentz and polarization effects and an empirical absorption correction based on ψ scan (North *et al.* 1968) was applied. Calculation were carried out with WINGX SYSTEM (Farrugia *et al.* 1999); the structure was solved with SIR97 (Altomare *et al.* 1999) and refined with SHELX97 (Sheldrick 1998). All non-hydrogen atoms except the sulfonic oxigens and the butane chain were refined anisotropically; hydrogen atoms were fixed in their calculated positions. The R factor based on F of observed reflections was 0.084 while the Rw based on F^2 for all reflections was 0.234 with $w = 1/[\sigma^2 F_o^2 + (0.1655P)^2$ where $P = (F_o^2 + 2F_c^2)/3$; goodness of fit on F^2 for all reflections was 0.914.

Table 1. Crystal data.

Empirical formula	$C_{22}\ H_{36}\ N_2\ O_5\ S$	
Formula weight	440.58	
Temperature	293(2) K	
Wavelength	0.71069 a	
Crystal system, space group	Triclinic, P1	
Unit cell dimensions	a = 35.270(5)Å	$\alpha = 90.0$ deg.
	b = 5.546(5) Å	$\beta = 93.2(2)$ deg.
	c = 11.931(5) Å	$\gamma = 90.0$ deg.
Volume	2330(2) $Å^3$	
Z, Calculated density	4, 1.253 Mg/m^3	
absorption coefficient	0.173 mm^{-1}	
F(000)	952	
Crystal size	0.2 × 0.2 × 0.4 mm	
Theta range for data collection	2.80 to 29.97 deg	
Limiting indices	$-7\leq h\leq 49$, $-7\leq k\leq 7$, $-16\leq l\leq 16$	
Reflections collected/unique	6934/6498 [R(int) = 0.035]	
Completeness to theta = 29.97	99.2%	
Refinement method	Full-matrix least-squares on F^2	
Data/restraints/parameters	6498/5/241	
Goodness-of-fit on F^2	0.914	
Final R indices [I>2sigma(I)]	$R_1 = 0.0836$, $wR_2 = 0.2338$	
R indices (all data)	$R_1 = 0.1902$, $wR_2 = 0.2705$	
Largest diff. peak and hole	0.834 and −0.464 e. $Å^{-3}$	

Spectroscopy

NMR spectra were obtained on a Bruker Avance AMX-400 spectrometer with a Broad Band 5 mm probe (inverse detection). Nominal frequencies are 100.13 and 400.13 MHz for ^{13}C and ^{1}H respectively. The typical acquisition parameters for ^{1}H are as follows: spectral bandwidth (SW) 10 ppm, pulse width 6.8 μs (90 ° pulse hard pulse on ^{1}H), pulse delay 0.5–1 s, number of scans (ns) 216–512. ^{13}C typical parameters: SW 200 ppm, pulse width 10 μs, ns 32 k. All spectra were collected at 300 K and referenced to TMS.

2D H,H-Homonuclear Correlated Spectroscopy (COSY) was performed according to Nagayama (Nagayama *et al.* 1980) and typical parameters were used. 2D H,X-Hetero Correlated Spectroscopy (HMQC and HMBC) experiments were performed implying 'Brüker' sequences 'inv4nd' (Bax *et al.* 1983) for evolution of $^{1}J_{HC}$ via heteronuclear zero and double quantum coherence, 'invbnd' for evolution of $^{1}J_{HC}$ via heteronuclear zero and double quantum coherence using BIRD sequence (Bax and Subramanian 1986), and 'inv4lplrnd' (Bax and Summers 1986) for evolution of $^{3}J_{HC}$ via heteronuclear zero and double quantum coherence, optimized on long range couplings, with low pass J-filter to suppress one-bond correlations. Typical averaged values of coupling constants are $^{1}J_{HC} = 145$ Hz and $^{3}J_{HC} = 7$ Hz, typical delay for inversion recovery optimized to give null for protons bound to ^{12}C, in BIRD sequence, is around 400 ms. pD values were corrected of 0.4 unit according to the relationship: pD = pH + 0.4 (Perrin *et al.* 1979).

^{1}H NMR titration of Tirofiban was performed on a D_2O millimolar solution, changing pD value by small addition of a saturated solution of NaOD in D_2O. The combine electrode was calibrated with standard buffer solution in H_2O (pH = 7.00 and pH = 4.01).

UV-spectrofotometric titrations were performed using a Perkin-Elmer Lambda 19 spectrophotometer at 25±0.1 °C in the 300–240 nm spectral range, employing 1 cm quartz cells. Cu(II)/Tirofiban and Co(II)/Tirofiban systems were investigated, maintaining [TirH] = 5×10^{-5} M and adding small amounts of $M(NO_3)_2$ in order to vary the metal to ligand molar ratio.

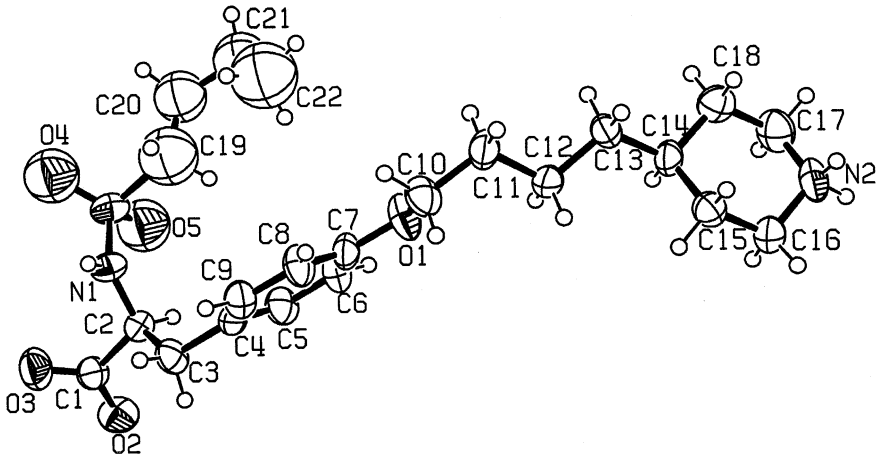

Fig. 1. ORTEP view of Tirofiban.

Table 4.

δH_2	δH_3	$\delta H_{3'}$	δH_5	δH_6	δH_8	δH_9	δH_{10}	δH_{11}	δH_{12}	δH_{13eq}	δH_{13ax}	δH_{14eq}	δH_{14ax}	δH_{15}	δH_{16}	δH_{17}	δH_{18}
4.21	3.29	2.86	7.35	7.05	4.14	1.83	1.54	1.42	1.67	2.01	1.41	3.46	3.01	2.77	1.45	1.22	0.83
δC_1	δC_2	δC_3	δC_4	δC_5	δC_6	δC_7	δC_8	δC_9	δC_{10}	δC_{11}	δC_{12}	δC_{13}	δC_{14}	δC_{15}	δC_{16}	δC_{17}	δC_{18}
176.37	58.69	37.39	130.02	131.09	115.30	157.60	68.86	28.63	22.41	34.98	33.14	28.63	44.45	52.73	24.87	21.07	13.02

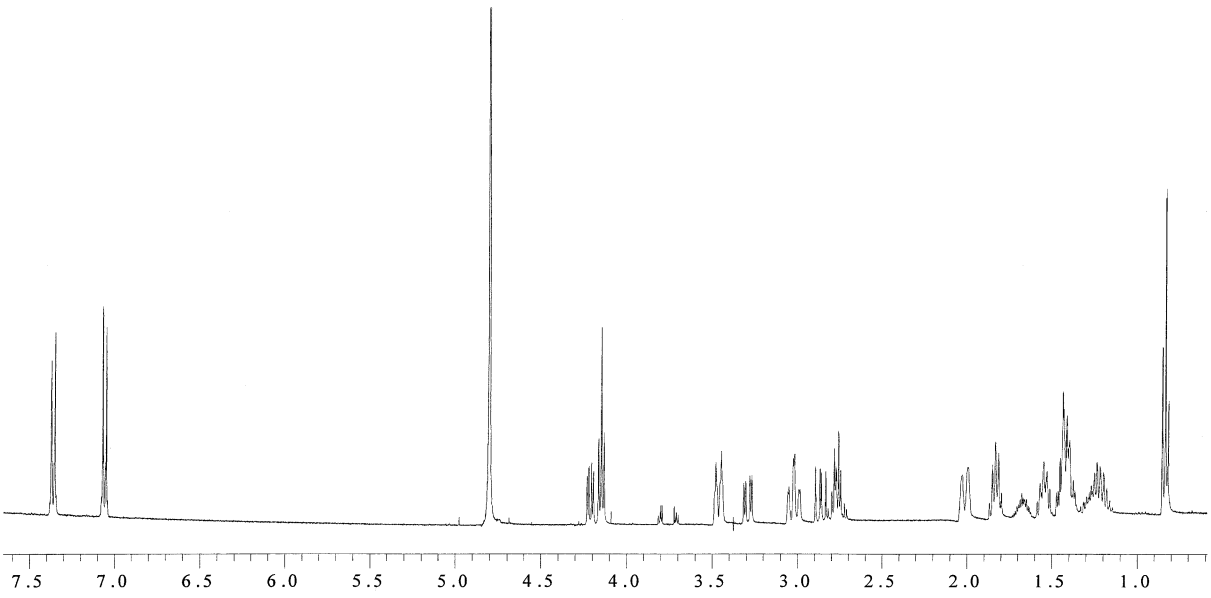

Fig. 2. ^{1}H NMR spectrum of Tirofiban in D_2O at 300 K.

Table 2. Bond distances (Å) and bond angles (deg).

C(1)-O(3)	1.206(6)	C(12)-C(13)	1.529(7)
C(1)-O(2)	1.257(6)	C(13)-C(14)	1.537(7)
C(1)-C(2)	1.539(7)	C(14)-C(18)	1.498(8)
C(2)-N(1)	1.458(6)	C(14)-C(15)	1.523(7)
C(2)-C(3)	1.505(6)	C(15)-C(16)	1.508(7)
C(3)-C(4)	1.529(6)	C(16)-N(2)	1.480(7)
C(4)-C(5)	1.367(7)	C(17)-N(2)	1.450(8)
C(4)-C(9)	1.389(7)	C(17)-C(18)	1.536(8)
C(5)-C(6)	1.385(7)	C(19)-C(20)	1.458(15)
C(6)-C(7)	1.365(8)	C(19)-S	1.919(11)
C(7)-O(1)	1.362(5)	C(20)-C(21)	1.547(15)
C(7)-C(8)	1.368(7)	C(21)-C(22)	1.504(17)
C(8)-C(9)	1.393(7)	N(1)-S	1.575(4)
C(10)-O(1)	1.436(7)	O(4)-S	1.424(8)
C(10)-C(11)	1.505(7)	O(5)-S	1.413(8)
C(11)-C(12)	1.516(7)		
O(3)-C(1)-O(2)	123.2(5)	C(12)-C(13)-C(14)	115.3(4)
O(3)-C(1)-C(2)	122.0(5)	C(18)-C(14)-C(15)	108.7(4)
O(2)-C(1)-C(2)	114.7(4)	C(18)-C(14)-C(13)	111.5(4)
N(1)-C(2)-C(3)	110.9(4)	C(15)-C(14)-C(13)	112.8(4)
N(1)-C(2)-C(1)	112.5(4)	C(16)-C(15)-C(14)	112.2(4)
C(3)-C(2)-C(1)	110.1(4)	N(2)-C(16)-C(15)	111.5(4)
C(2)-C(3)-C(4)	114.8(4)	N(2)-C(17)-C(18)	111.2(5)
C(5)-C(4)-C(9)	118.0(4)	C(14)-C(18)-C(17)	111.5(5)
C(5)-C(4)-C(3)	120.1(4)	C(20)-C(19)-S	113.2(11)
C(9)-C(4)-C(3)	121.9(4)	C(19)-C(20)-C(21)	116.1(15)
C(4)-C(5)-C(6)	121.1(5)	C(22)-C(21)-C(20)	112(2)
C(7)-C(6)-C(5)	120.7(5)	C(2)-N(1)-S	122.9(3)
O(1)-C(7)-C(6)	115.5(4)	C(17)-N(2)-C(16)	113.6(4)
O(1)-C(7)-C(8)	125.0(5)	C(7)-O(1)-C(10)	118.7(4)
C(6)-C(7)-C(8)	119.5(4)	O(5)-S-O(4)	129.7(5)
C(7)-C(8)-C(9)	119.8(4)	O(5)-S-N(1)	108.7(4)
C(4)-C(9)-C(8)	120.9(4)	O(4)-S-N(1)	108.5(4)
O(1)-C(10)-C(11)	107.1(4)	O(5)-S-C(19)	104.8(5)
C(10)-C(11)-C(12)	114.8(4)	O(4)-S-C(19)	102.4(5)
C(11)-C(12)-C(13)	111.6(4)	N(1)-S-C(19)	97.8(5)

Table 3. Possible hydrogen bonds.

N2 – H2B	N2...O3^{I}	H2B....O3^{I}	N2 – H2B...O3^{I}
0.90(1)	2.747(7)	1.879(5)	161.2(3)
N2 – H2A	N2...O2^{II}	H2A...O2^{II}	N2 – H2A...O2^{II}
0.90(1)	2.766(6)	1.975(4)	145.8(3)
N1 – H1	N1...O2^{III}	H1...O2^{III}	N1 – H1...O2^{III}
0.86(1)	2.7915(6)	2.069(4)	167.5(3)

I) x+1/2, y+1/2, z
II) x1/2, y−1/2, z
III) x, y−1, z

The infrared spectra of the solid compounds in KBr pellets were obtained by means of a Perkin-Elmer FT-IR 1600, in the 4000–400 cm^{-1} spectral range.

Results

Description of the structure

Bond distances and angles are reported in Table 2, with the atom numbering as in Figure 1. The structure consists of one independent Tirofiban molecule. The C-O carboxylic bond lengths are very similar suggesting that the carboxylic group is in the anionic form. On the other hand, piperidine molecule appear in the protonated form and shows the usual 'chair' conformation with torsion angles of 53.8° and 56.1°. The sulfonamidic nitrogen shows an sp^2 hybridization, and the S-N distance is comparable with those found in $ArSO_2$ N-protected amino acids (Iacopino *et al.* 1999). The phenyl ring of the tyrosine moiety is planar with max deviation from the plane of 0.02 Å. Both nitrogen atoms are involved in a network of hydrogen bonds with carboxylic oxygens in the x-y plane (Table 3). Crystal packing is completed by ring-stacking interactions involving phenyl rings along y axis (range 3.59–3.83 Å). The poor quality of the structure is mainly due to the great disorder of the butane chains together with sulfonic oxygens.

NMR spectroscopy

Tirofiban shows quite a complicate spectral pattern, in fact the region between 4.3 and 1 ppm is crowded by almost all proton signals. The backbone of the molecule is constituted by tyrosine and the complete assignment for both proton and carbon is given by means of homo and heteronuclear correlated spectroscopy. Scheme 1 reports Tirofiban while Figure 2 and Table 4 report its NMR signals assignment. As shown in ^{1}H NMR spectrum the unequivalence of β protons in tyrosine block makes α proton a double doublet. H_{13} and H_{14} have a particular spectral pattern, whose spectral width enlargement is probably due to a relaxation phenomenon related to dipolar interaction with piperidine nitrogen.

pH-metric titration of Tirofiban in D_2O solution clearly shows the pH dependence of many resonances, like H_2, H_3, $H_{3'}$, H_{13}, H_{14}, as illustrated in Figure 3, suggesting deprotonation processes. H_2 and H_3 protons show two different equivalent points (Figure 4) related to carboxylic and sulfonamidic deprotonation,

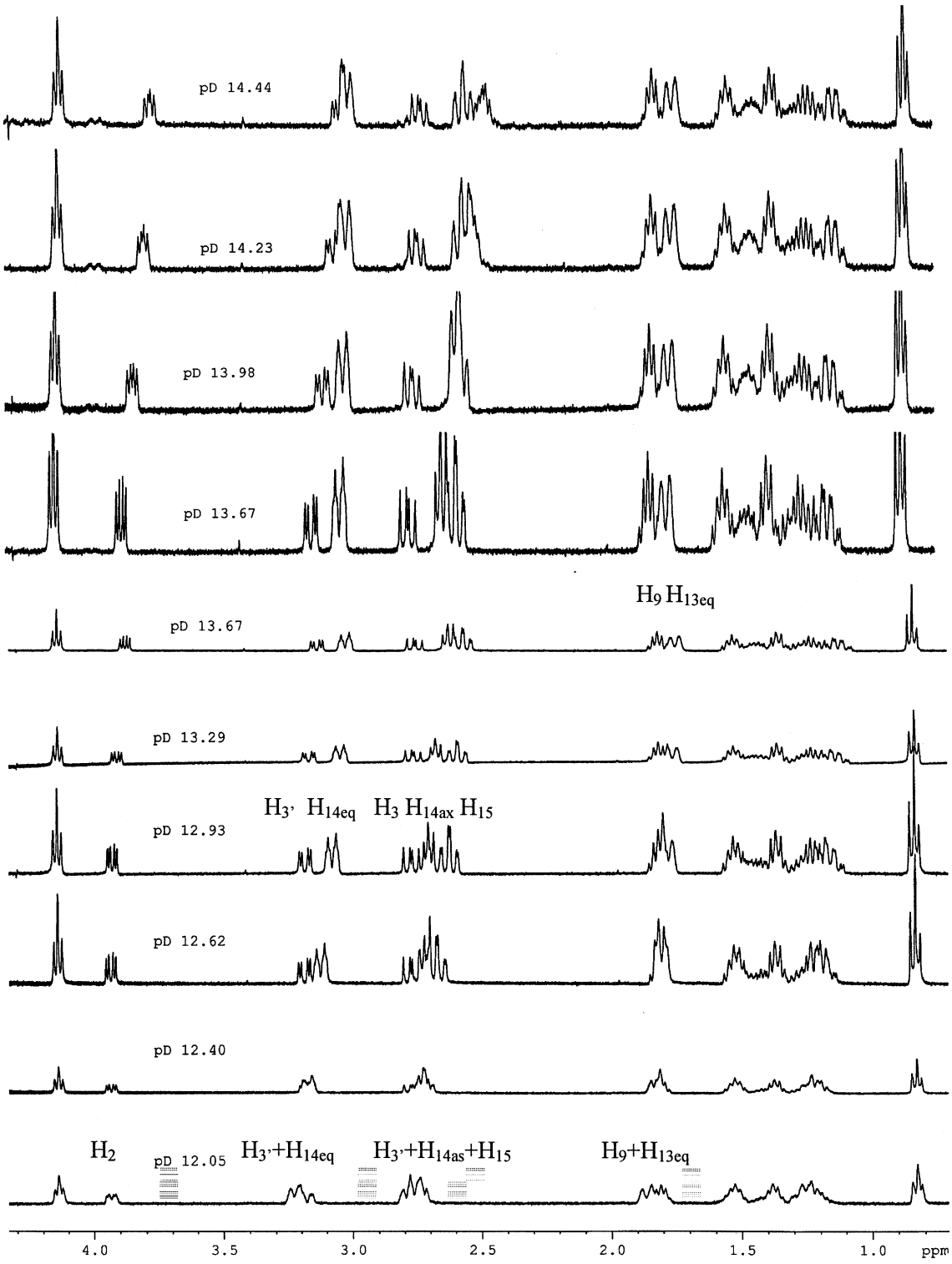

Fig. 3. -^{1}H NMR spectra of Tirofiban at increasing pD value.

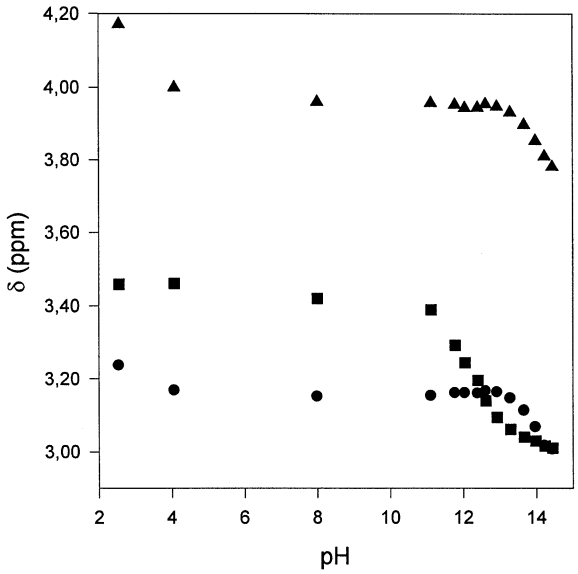

Fig. 4. pH dependence of ^{1}H NMR resonances of H_2(▲) H_3(●) and H_{13}(■).

similarly to other N-protected sulfonyl amino acids. The deshielding effect due to the negative charge during the deprotonation process induces an upfield shift. While H_2 undergoes a similar shift for both carboxylic and sulfonamidic deprotonation processes, H_3 and $H_{3'}$ feel more strongly the equilibrium of the sulfonamidic nitrogen than the carboxylic one. H_{13} and H_{14} protons show instead only one equilibrium, corresponding to the piperidine nitrogen deprotonation. All the equilibria are attained rapidly in the NMR time scale, such that the chemical shift for proton is a concentration-weighted average over both the chemical species (protonated and not) in which the nucleus is present. Plotting δ vs. pH a titration curve is obtained as shown in Figure 4; equilibrium constants and pKa values are refined by HYPNMR (Frassineti *et al.* 1995), and are consistent with those calculated by means of potentiometry, three pK_a are found: $pKa_{COOH} = 3.1(1)$, $pKa_{NHPIP} = 11.6(1)$ and $pKa_{NHSO2} = 13.8(1)$.

Addition of bivalent metal ions such as Cd(II), Pb(II) or Ca(II) doesn't effect any signal and, when pD is increased, the precipitation of the complex species is observed in different solvent media (D_2O, CD_3OD, DMSO), the insolubility of the compounds make it impossible to acquire any spectra.

Potentiometry

By means of potentiometric titrations two dissociation steps are found in Tirofiban involving the carboxylic

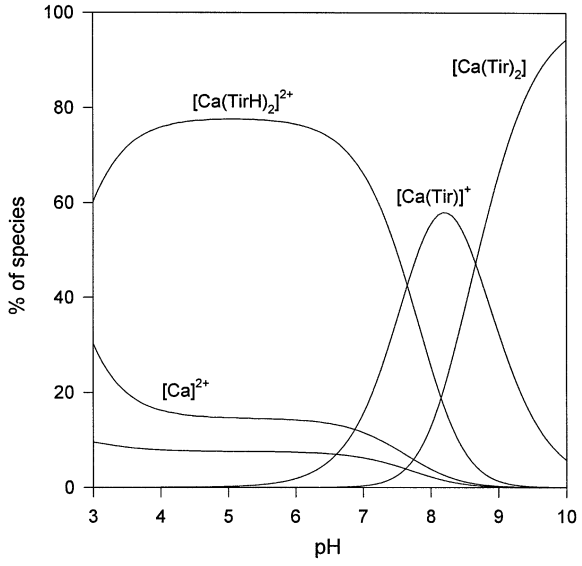

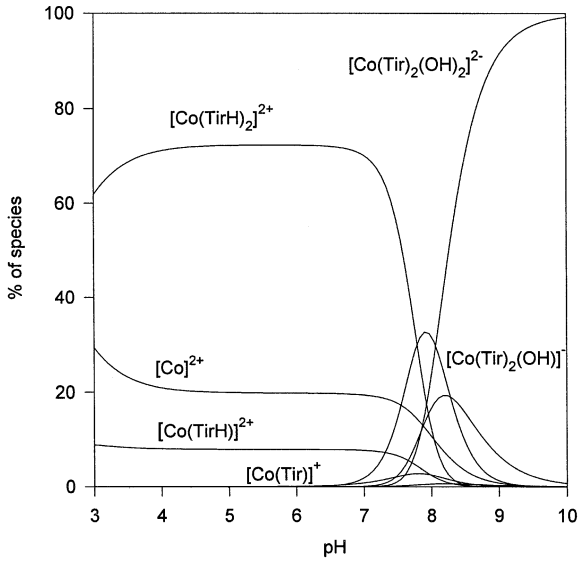

Fig. 5. Species distribution curves for Ca(II)-Tirofiban and Co(II)-Tirofiban systems, in function of pH, [M] = 0.001 M.

group and the piperidinic nitrogen with $pK_{a1} = 3.06(2)$ and $pK_{a2} = 11.06(3)$, respectively.

The pK_{a1} of the carboxylic group is smaller compared to those found in other N-Acetyl or N-benzoyl amino acids (range 3.35–3.80) (Menabue *et al.* 1998), while is near the one found for other N-arylsulfonyl amino acids (Saladini *et al.* 2000). The pK_{a2} of piperidinic nitrogen is near to that found by NMR and to that of piperidine (11.1) (NIST). There is no hint

Table 5. Logarithms of stability constants of complex species at 25 °C and I = 0.1 M.

			Cu(II)	Ni(II)	Co(II)	Cd(II)	Pb(II)	Zn(II)	Ca(II)
TirH	$Log\beta_{011}$	11.06(3)							
$TirH_2^+$	$Log\beta_{012}$	14.12(2)							
$[M(TirH]^{2+}$	$Log\beta_{111}$		13.7	13.4	14.0	14.4	14.3	13.7	13.40
	$LogK_1$*		2.6	2.3	2.9	3.3	3.2	2.6	2.3
$[M(Tir)]^+$	$Log\beta_{110}$		8.3	5.6	6.0			6.5	6.8
[M(Tir)(OH)]	$Log\beta_1 1-1$		−1.2	−3.3	−2.6		2.45	−0.1	
$[M(TirH)_2]^{2+}$	$Log\beta_{112}$		27.7	28.5	29.3	29.1	28.6	29.0	28.1
	$LogK_2$*		5.6	6.4	7.2	7.0	6.5	6.9	6.0
$[M(Tir)_2]$	$Log\beta_{120}$		16.6		13.7		17.1	13.9	11.8
$[M(Tir)_2(OH)]^-$	$Log\beta_{12-1}$				5.5				
$[M(Tir)_2(OH)_2]^{2-}$	$Log\beta_{12-2}$				−2.4				

*$LogK_1 = Log\beta_{011}$ and is referred to the equilibrium M^{2+}+TirH↔$[M(TirH)]^{2+}$
Log $K_2 = Log\beta_{112} - 2Log\beta_{011}$ and is referred to the equilibrium $M^{2+} + 2TirH \leftrightarrow [M(TirH)_2]^{2+}$

of sulfonamidic nitrogen deprotonation from potentiometric data, contrarily to what happens in $ArSO_2$-N- protected amino acids, where the presence of the phenyl ring enhances the acidity of the NH group, lowering it's pKa to the range of 11.3–12.0 (Saladini *et al*. 2000). The value of sulfonamidic pKa of 13.8(2), found by means of NMR analysis, is in line with those of amidic nitrogen (NIST).

The potentiometric titrations of all metal-to-ligand molar ratios investigated are quite superimposable to that of Tirofiban up to pH 4, suggesting that no significant complex formation takes place before almost complete ionization of carboxylic group. After the equivalent point, corresponding to the complete dissociation of the carboxylic group, the precipitation of metal hydroxide take places at a pH value depending from the stability of the Me(II)-hydroxo species (NIST). In the Cd(II) containing system the precipitation of $[Cd(Tir)_2] \cdot 2HCl$ occurs while in the Hg(II) containing system, the precipitation of the solid complex $[Hg(Tir)_2] \cdot 2HCl$ is observed yet from pH 4.5, preventing potentiometric analysis.

The logarithm of the overall stability constants of the complex species are reported in Table 5, and species distribution curves for Ca(II) and Co(II) containing systems are shown in Figure 5. The prevailing species is $[M(TirH)_2]^{2+}$ (TirH = neutral Tirofiban with carboxylic group in the dissociated form and protonated piperidinic nitrogen) where the ligand coordinates the metal ion through carboxylic group, while the piperidinic nitrogen is still protonated. Increasing pH, the formation of $[M(Tir)]^+$ or $[M(Tir)_2]$ species is observed where piperidinic nitrogen undergoes deprotonation at a pH value lower than in the free ligand. The lowering of pK_{a2} induced by metal ion suggests a possible involvement of piperidinic nitrogen in metal coordination, with the formation of insoluble polymeric species. In the same time mixed hydroxo complexes are formed, followed by the precipitation of metal hydroxide, as the solubility limit is reached.

This carboxylate type coordination is the one normally found in presence of R-CO-N protected aminoacids, like acetyl or benzoyl aminoacids, irrespectively of the R group, while the deprotonation and metal coordination of aminoacidic nitrogrn is never found in these systems. Nevertheless $LogK_1$ value for $[Ca(TirH)]^{2+}$ species (Table 5) is considerably higher than those found in Cu(II)-N-acetyl or benzoylglycine systems [$logK_1$ 0.29 and 0.43, respectively (NIST)].

$Log\beta_{111}$ and $Log\beta_{122}$ for all metal ions investigated are also greater than the corresponding values in presence of N-(2-nitrophenylsulfonyl)glycine (mean $Log\beta_{111} = 12.6$; mean $Log\beta_{122} = 25.9$) (Saladini *et al*. 2000). Concerning Ca(II) containing system the $LogK_1$ and $LogK_2$ values are higher than those with simple carboxylic acids, even also higher than those found with α-hydroxocarboxylic acids (mean value for $logK_1 = 1.9$) and with sugar acids like Galactaric Acid ($logK_1 = 2.45$) (Saladini *et al.* 2001).

The great stability of our complexes may be due to intermolecular hydrophilic interactions of Tirofiban, i.e. hydrogen bonds, involving both nitrogen atoms and carboxylic oxygens, as well as the formation of hydrophobic interactions, like stacking interactions

Table 6. More relevant IR bands and their tentative assignment (*stretching band of the aminoacidic NH).

	TirHCl	$[Hg(Tir)_2] \cdot 2HCl$	$[Cd(Tir)_2] \cdot 2HCl$
ν(NH)*	3450b	3442b	3490b
$\nu(NH_2^+)$	3151s	3148s	3265s, 3126s
ν(CH)	2936vs, 2861	2935vs, 2868s	2935vs, 2868s
ν(OCO)asym	1652vs	1610-1582vs	1621vs
δ(NH)	1514vs	1514vs	1515vs
ν(OCO)sym	1430s	1391s	1382s
$\Delta\nu$	221	219	239
$\nu(SO_2)$asym	1329s	1298s	1294s
$\nu(SO_2)$sym	1146s	1140s	1138s

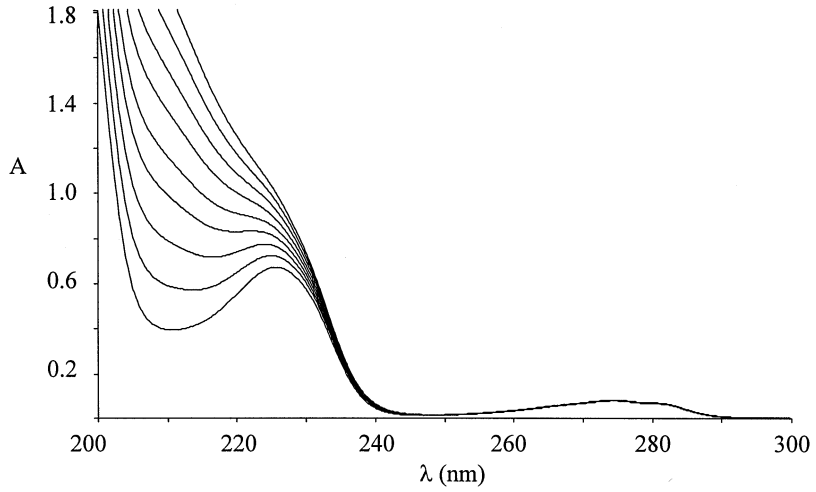

Fig. 6. Spectra of Tirofiban-Co(II) system at different ligand-to-metal molar ratios: 1:0.2, 1:0.3; 1:0.4; 1:0.5; 1:0.7; 1:0.8; 1:1; 1:1.5 1:2 at increasing absorbance; Tirofiban is 5×10^{-5} M.

involving phenyl ring of the tyrosine residue of the coordinated molecules, as observed in the solid state. The great affinity of Tirofiban for various bivalent metal ions, among which Ca(II), is probably related to the increased antiplatelet efficacy of Tirofiban on decreasing plasma Ca(II) levels.

Spectroscopic analysis

UV spectrum of Tirofiban shows a band maximum at $\lambda = 225$ nm ($\epsilon = 1.3 \times 10^4$) and a band maximum at $\lambda = 278$ nm ($\epsilon = 1.5 \times 10^3$) that is typical of tyrosine. Increasing pH the band maximum at 225 doesn't change in position while the absorbance increases but no titolative trend is observed. The addition of different amounts of metal ion to the solution of Tirofiban leads to an increasing of the absorbance at 225 nm with a loss of resolution of the maximum until it disappears when the 1:1 metal to ligand molar ratio is reached. This behavior is indicative of the coordination of Tirofiban to the metal ion; increasing pH no further spectral changes are observed. Figure 6 reports the spectra of the Co(II)-Tirofiban system at different metal to ligand molar ratios.

In Table 6 the more relevant IR bands with their tentative assignment are shown. In Tirofiban the stretching band of the aminoacidic NH is observed at 3450 cm^{-1}, while in the region 3100–2860 cm^{-1} the stretching frequencies of the piperidinic NH_2^+ falls, according with secondary amine hydroalides, involved in strong hydrogen bonds (Colthrum *et al.* 1964; Bellamy *et al.* 1975) as observed in the crystal structure. The presence of strong hydrogen bonds is also suggested by the low energy of the NH bending mode that falls to 1514 cm^{-1}.

In the Cd(II) complexe these bands are shifted to higher energy, therefore not excluding the metal coordination of the aminic group in the solid complexes. The carboxylic group in Tirofiban shows also to bands: an intense antisymmetric carboxylate stretching and a symmetric one, according to the dissociated OCO group as shown by the crystal structure. The same behaviour is observed in the complexes suggesting a bidentate coordination mode of the carboxylic group as $\Delta\nu(\nu(\mathrm{OCO})_{\mathrm{asym}} - \nu(\mathrm{OCO})_{\mathrm{sym}})$ is of the same magnitude as in the free ligand.

The position of the stretching frequencies of SO_2 group are almost unchanged in the metal complexes with respect to Tirofiban, excluding any involvement of SO_2 group in metal coordination.

Supplementary material

Crystallographic data (excluding structure factors) have been deposited with the Cambridge Crystallographic Data Center as supplementary publication no. CCDC 205352 and can be obtained free of charge on application to the CCDC, 12 Union Road, Cambridge CB2 1EZ, U.K. [Fax: +44-1223/336-033; E-mail: deposit@ccdc.cam.ac.uk].

Acknowledgements

We are grateful to Merck Sharpe & Dohme which supplied Tirofiban, to the Centro Interdipartimentale Grandi Strumenti (CIGS) of the University of Modena and Reggio Emilia which supplied the diffractometer and the NMR spectrometer, we are also thankful to the Ministero dell'Università e della Ricerca Scientifica e Tecnologica of Italy for financial support.

Synopsis

The crystal structure of Tirofiban [N-(n-butanesulfonyl)-O-(4-(4-piperidinyl)-butyl)-(S)-tyrosine] is reported togehter with its H NMR and potentiometric characterisation. The metal(II) coordination ability is also tested by means of spectroscopic and potentiometric measurements.

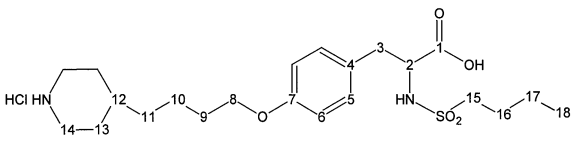

References

Altomare A, Burla MC, Cavalli M, Cascarano GL, Giacovazzo C, Gagliardi A, Moliterni AGG, Polidori G, Spagna R. 1999 *SIR*97: A new tool for crystal structure determination and refinement. *J Appl Cryst* **32** 115–119.

Battistuzzi G, Borsari M, Menabue L, Saladini M, Sola M. 1996 Amide group coordination to the Pb^{2+} ion. *Inorg Chem* **35**, 4239–4246.

Bax A, Griffey RH, Hawkins BL. 1983 Correlation of proton and nitrogen-15 chemical shifts by multiple quantum NMR*. *J Magn Reson* **55**, 301–315.

Bax A, Summers MF. 1986 Proton and carbon-13 assignments from sensitivity-enhanced detection of heteronuclear multiple-bond connectivity by 2D multiple quantum NMR. *J Am Chem Soc* **108**, 2093–2094.

Bax A, Subramanian S. 1986 Sensitivity-enhanced two-dimensional heteronuclear shift correlation NMR spectroscopy. *J Magn Reson* **67**, 565–569.

Bellamy LJ. 1975 The infrared Spectra of Complex Molecules. London: Chapman and Hall.

Borsari M, Menabue L, Saladini M. 1999 Coordination properties of N-*p*-tolylsulfonyl-L-glutamic acid toward metal(II). Part 2. Solution study on binary and ternary 2,2′-bipyridine containing systems. *Polyhedron* **18**, 1983–1989.

Colthrum NB, Daly LH, Wiberley SE. 1964 Introduction to Infrared and Raman Spectroscopy. New York: Academic Press.

Chung JYL, Zhao D, Hunghes DL, Grabowski EJJ 1993 A practical synthesis of fibrogen receptor antagonist MK-383. Selective functionalization of (S)-tyrosine. *Tetrahedron* **49**, 5767–5776.

Farrugia LJ. 1999 *WinGX* suite for small-molecule single-crystal crystallography. *J Appl Cryst* **32**, 837–838.

Ferguson JJ, Lau TK 1998 New antiplatelet agents for acute coronary syndromes. *Am Heart* **135**, S194–200.

Frassineti C, Ghelli S, Gans P, Sabatini A, Moruzzi MS, Vacca A. 1995 Nuclear magnetic resonance as a tool for determining protonation constants of natural polyprotic bases in solution. *Anal Biochem* **231**, 374–382.

Gans P, Sabatini A, Vacca A. 1996 Investigation of equilibria in solution. Determination of equilibrium constants with the HYPERQUAD suite of programs. *Talanta* **43**, 1739–1753.

Kazunao K, Kazuo U. 2002 Clinical Pharmacokinetics of Tirofiban, a Nonpeptide Glycoprotein IIb/IIIa Receptor Antagonist: Comparison with the Monoclonal Antibody Abciximab. [Review] *Clin Pharmacok* **41**(3) 187–195.

Kereiakes DJ, Lorenz T, Young JJ, Kukielka G, Mueller MN, Nanniazzi-Alaimo L, Phillips DR 2001 Differential effects of citrate *versus* PPACK anticoagulation on measured platelet inhibition by Abciximab, Eptifibatide and Tirofiban. *J Thromb Thrombolys* **12**, 123–127.

Iacopino D, Menabue L, Saladini M. 1999 Crystallographic study on metal(II) complexes with N-(2-Nitrophenylsulfonyl)glycine. *Aust J Chem* **52**, 741–748.

McClellan KJ, Goa KL 1998 Tirofiban: A review of its use in acute coronary syndromes. *Drugs* **56**, 1067–1080.

Menabue L, Saladini M, Bavoso A, Ostuni A. 1998 Investigation on coordination ability of N-chloro-acetylglycine towards Cu(II) in solid and solution state. *Inorg Chim Acta* **268**, 205–210.

Mousa SA, Bozarth JM, Forsythe MS, Slee A. 2000 Differential antiplatelet efficacy for various GPIIb/IIIa antagonists: role of plasma calcium levels. *Cardiov Res* **47**, 819–826.

Nagayama, K, Kumar A, Wuethrich K, Ernst RR. 1980 Experimental techniques of two-dimensional correlated spectroscopy. *J Magn Reson* **40**, 321–334

NIST Standard Reference database 46, Critically selected Stability Constants, Version 5, webbook.nist.gov.

North AC, Phillips DC, Mathews FS. 1968 A semi-empirical method of absorption correction *Acta Crystallogr Sect A* **24**, 351–359.

Perrin DD, Dempsey B. 1979 *Buffers for pH and Metal Ion Control*. London: Chapman and Hall.

Saladini M, Iacopino D, Menabue L. 2000 Metal(II) binding ability of a novel N-protected amino acid. Solution state investigation on binary and ternary complexes with 2,2′-bipyridine. *J Inorg Biochem* **78** 355–361 and ref. therein.

Saladini M, Menabue L, Ferrari E, Iacopino D. 2001 Amide group coordination to the Hg^{2+} ion. Potentiometric, ^{1}H-NMR and structural study on Hg^{2+}-N-protected amino acids systems. *J Chem Soc Dalton Trans* 1513–1519.

Saladini M, Menabue L, Ferrari E. 2001 Sugar complexes with metal^{2+} ions: thermodynamic parameters of associations of Ca^{2+}, Mg^{2+} and Zn^{2+} with galactaric acid. *Carbohydr Res* **336** 55–61.

Sheldrick GM. 1998 SHELX97 Programs for Crystal Structure Analysis Institute für Anorganische Chemie der Universitat, Gottingen, Germany.

Van de Werf F. 1997 Clinical trials with glycoprotein IIb/IIIa receptor antagonists in acute coronary syndromes. *Tromb Haemost* **78**, 210–213.